HHS Public Access

Author manuscript

Neurobiol Aging. Author manuscript; available in PMC 2018 October 01.

Published in final edited form as:

Neurobiol Aging. 2017 October ; 58: 1–13. doi:10.1016/j.neurobiolaging.2017.06.003.

CENTRAL INSULIN DYSREGULATION AND ENERGY DYSHOMEOSTASIS IN TWO MOUSE MODELS OF ALZHEIMER'S DISEASE

Ramon Velazquez[1], **An Tran**[1], **Egide Ishimwe**[2], **Larry Denner**[3], **Nikhil Dave**[1], **Salvatore Oddo**[1,4,*,#], and **Kelly T Dineley**[2,*,#]

[1]Arizona State University-Banner Neurodegenerative Disease Research Center at the Biodesign Institute, Arizona State University, Tempe, AZ, 85287

[2]Department of Neurology, Mitchell Center for Neurodegenerative Diseases, University of Texas Medical Branch at Galveston (UTMB), Galveston, TX, 77555

[3]Internal Medicine, Mitchell Center for Neurodegenerative Diseases, University of Texas Medical Branch at Galveston (UTMB), Galveston, TX, 77555

[4]School of Life Sciences, Arizona State University, Tempe, Arizona, 85287

Abstract

Alzheimer's disease (AD) is the most prevalent neurodegenerative disorder worldwide. While the causes of AD are not known, several risk factors have been identified. Among these, type 2 diabetes (T2D), a chronic metabolic disease, is one of the most prevalent risk factors for AD. Insulin resistance, which is associated with T2D, is defined as diminished or absent insulin signaling, and is reflected by peripheral blood hyperglycemia and impaired glucose clearance. In this study, we used complimentary approaches to probe for peripheral insulin resistance, central nervous system (CNS) insulin sensitivity and energy homeostasis in Tg2576 and 3xTg-AD mice, two widely used animal models of AD. We report that CNS insulin signaling abnormalities are evident months before peripheral insulin resistance. Additionally, we find that brain energy metabolism is differentially altered in both mouse models, with the 3xTg-AD mice showing more extensive changes. Collectively, our data suggest that early AD may reflect engagement of different signaling networks that influence CNS metabolism, which in-turn may alter peripheral insulin signaling.

[*]To whom correspondence should be addressed: Salvatore Oddo, Ph.D., Neurodegenerative Disease Research Center, Biodesign Institute, School of Life Sciences, Arizona State University, 1001 S MacAllister Ave, Tempe, AZ 85287, 480-727-3490, oddo@asu.edu. Kelly Dineley, Ph.D., Department of Neurology, Mitchell Center for Neurodegenerative Diseases, University of Texas Medical Branch at Galveston, Galveston, TX, 77555-0616, 409-747-7060, ktdinele@utmb.edu.
[#]These authors share senior authorship

Conflicts

The authors report no conflicts of interest.

1. Introduction

Alzheimer's disease (AD) is the most prevalent neurodegenerative disorder worldwide. Clinically, AD is characterized by impairments of memory and cognitive functions that affect a person's ability to perform activities of daily living (Alzheimer's Association, 2016; LaFerla and Oddo, 2005). Accumulation of amyloid-β (Aβ) and neurofibrillary tangles are the prominent neuropathologies in AD patients (Querfurth and LaFerla, 2010). Currently, 5.4 million Americans are affected by AD, and this number is expected to rise to 13.8 million by 2050 (Alzheimer's Association, 2016). Several genetic and environmental risk factors (APOE4 inheritance, Down syndrome, age, education, lifestyle, etc.) contribute to the prevalence of AD (Alzheimer's Association, 2016; Grober et al., 2008; Head et al., 2016; Kivipelto et al., 2002; Moll et al., 2014; Wiseman et al., 2015).

Type 2 diabetes (T2D), one of the most prevalent risk factors for AD, is a chronic metabolic disease that currently affects 21 million Americans (Alex et al., 2012). Peripheral insulin resistance, a defining feature of T2D, is reflected by fasting levels of hyperglycemia and impaired glucose clearance in the glucose tolerance test (Boura-Halfon and Zick, 2009a; Jackson et al., 2017). Insulin resistance manifests as disrupted coupling of insulin and insulin receptor signaling mediators (Dineley et al., 2014; Gual et al., 2005; Steen et al., 2005; Tanti and Jager, 2009).

In the CNS, insulin impinges upon its receptor to activate insulin signaling and the expression of genes that modulate memory (Dineley et al., 2014; Watson and Craft, 2004). Compelling evidence suggests that insulin resistance and T2D worsen AD pathology and cognitive deficits (Haan, 2006; Ramos-Rodriguez et al., 2016; Saedi et al., 2016; Sena et al., 2015; Sheen and Sheu, 2016; Zilliox et al., 2016). To this end, central insulin signaling dysregulation has been demonstrated in post-mortem hippocampal and cortical samples from subjects with both mild cognitive impairment (MCI) and early AD (Talbot et al., 2012a; Watson and Craft, 2004). The insulin receptor (IR), the insulin receptor substrate-1 (IRS-1), the phosphoinositide-dependent kinase-1 (PDK1), and the alpha serine/threonine-protein kinase (AKT) are regulated through stoichiometric activation/inactivation phosphorylation profiles and form the components of a highly integrated intracellular insulin signaling pathway that undergoes diminished function in AD (Boura-Halfon and Zick, 2009a; Galbo et al., 2013, 2011; Gual et al., 2005; Long-Smith et al., 2013; Steen et al., 2005; Stuart et al., 2014; Talbot et al., 2012; Wang et al., 2009; Yarchoan and Arnold, 2014; Zhang et al., 2016).

Importantly, although dysfunction in central insulin signaling is evident in MCI and AD patient post-mortem hippocampal and cortical tissue, it is not certain whether these changes may occur before or after peripheral insulin resistance. While evidence suggests that insulin resistance and T2D worsen AD pathology, it is not presumed that all AD patients have peripheral insulin resistance prior to AD diagnoses. To this end, parsing out the relative contribution of central and peripheral insulin resistance to dementia and diabetes may lead to novel targets and treatments.

The development of preclinical AD animal models has strengthened the notion that insulin resistance, T2D, and AD are mechanistically linked (Goldstein et al., 2007; Ho et al., 2004; Pedersen and Flynn, 2004; Rodriguez-Rivera et al., 2011). For example, Tg2576 mice exhibit increased body weight, fasting hyperglycemia and hyperinsulinemia. These changes are accompanied by peripheral insulin resistance by 9 months of age (as measured by the GTT), which coincides with the onset of Aβ accumulation in the brain (Hsiao et al., 1996; Pedersen and Flynn, 2004; Rodriguez-Rivera et al., 2011). Further, 14-month-old female 3xTg-AD mice develop insulin resistance, fasting hyperinsulinemia and hyperglycemia (Vandal et al., 2015). The link between insulin resistance and AD is further strengthened by data showing that diet-induced insulin resistance exacerbates Aβ accumulation, tau phosphorylation and cognitive impairments, and leads to the development of a diabetes-like phenotype (Cao et al., 2007; Carvalho et al., 2012; Orr et al., 2014). Thus, numerous previous studies strongly suggest that AD pathology begets a diabetes-like phenotype; however, the temporal relationship between CNS insulin signaling dysregulation and peripheral insulin resistance remains unexplored.

Herein, we report results from studies monitoring the total and phosphorylation status of several key components of the insulin signaling pathway in Tg2576 and 3xTg-AD mice at ages prior to and coincident with amyloid deposition. We found evidence that CNS insulin signaling dysregulation precedes the onset of peripheral insulin resistance in both Tg2576 and 3xTg-AD mice that progresses with age. In contrast, alterations in markers of energy homeostasis were detected only after the onset of both central and peripheral insulin deficits. Thus, the common pathology between the two models, aberrant Aβ misfolding and accumulation appears capable of driving CNS insulin signaling dysregulation as well as peripheral insulin resistance. However, in 3xTg-AD mice markers for CNS insulin resistance manifest earlier relative to peripheral insulin resistance and progress more aggressively suggesting that discrepancies between Tg2576 and 3xTg-AD CNS insulin signaling may be the result of 3xTg-AD genetically-driven tau pathology.

2. Methods & Materials

2.1 Animals

Tg2576 mice were bred by mating heterozygous Tg2576 males, negative for the retinal degeneration (rd) gene, with C57Bl6/SJL (F1) females (Stock No. 100012, Jackson Laboratory) and genotyped as described in (Jahrling et al., 2014). Details for the generation and genotyping of 3xTg-AD mice used in the current study were previously reported (Oddo et al., 2003). Age-matched wildtype (WT) mice served as controls for both lines of AD preclinical animal models. Tg2576 and 3xTg-AD mice were housed in the University of Texas Medical Branch (UTMB) and Arizona State University Animal Resource Center Facilities, respectively. These facilities operate in compliance with the USDA Animal Welfare Act, the Guide for the Care and Use of Laboratory Animals, under OLAW accreditation, and IACUC approved protocols. Mice were housed up to 5 per cage, with *ad libitum* access to food and water.

Within the 3xTg-AD colony, male mice show high neuropathological variability, even between littermates. In contrast, female 3xTg-AD mice do not show such large variability

and their phenotype progresses with age in a predictable manner. Therefore, only female 3xTg-AD mice were used for the experiments described herein. Experimenters were blinded to genotype during key data acquisition and analysis steps.

2.2 Glucose tolerance test

Tg2576 glucose tolerance data have been published illustrating peripheral insulin resistance at 9 months of age but not at 5 months of age (Rodriguez-Rivera et al., 2011). Here, we examined glucose tolerance only in 3xTg-AD mice as previously described (Orr et al., 2014; Rodriguez-Rivera et al., 2011). Specifically, 3xTg-AD mice were overnight fasted for 16 hours, then were weighed the following morning prior to nicking tails with a fresh razor blade to measure baseline fasting blood glucose level. All animals received 2 mg/kg glucose injection into the intraperitoneal (i.p.) cavity. At 15, 30, 45, 60, 90, 120 and 210 minutes post-injection, blood glucose was sampled from the tail using a TRUEtrack glucose meter and TRUEtrack test strips (Trividia Health, Fort Lauderdale, FL).

2.3 Immunoblot

Immunoblots were performed on Tg2576 and 3xTg-AD brain homogenates using our previously described methods (Caccamo et al., 2015; Denner et al., 2012; Dineley et al., 2001; Sando et al., 2011; Velazquez et al., 2016). Of note, Tg2576 hippocampal tissue was analyzed, while hippocampal and cortex combined homogenates were used for 3xTg-AD mice. We focused on the Tg2576 hippocampus as plaque pathology is not yet apparent at 5 months of age and starts to develop at 9 months of age; however, these mice exhibit spatial, hippocampal-dependent learning and memory deficits at these ages (Ashe, 2006; Rodriguez-Rivera et al., 2011). 3xTg-AD mice develop a global neurobehavioral phenotype, providing our rationale for investigating the cortex and hippocampus (Oddo et al., 2003). Equivalent amounts of protein extract (DC Protein Assay, Bio-Rad) were resolved by SDS-PAGE, transferred to PVDF membrane (Immobilon, Millipore) or nitrocellulose membranes (iBlot2, Life Technologies), and probed with the appropriate primary and secondary antibodies. The amount of protein loaded was chosen to ensure band intensities were in the linear range (10–40 μg depending on the protein of interest) for densitometry. Equivalent loading was determined by appropriate loading controls as described in the figure legends.

Western blots of proteins extracted from Tg2576 mice were detected by chemiluminescence (Advance ECL, GE Healthcare). Film exposures in the linear range for the antigen-antibody combination were developed with a Kodak imager (Kodak), scanned at 300 dpi, then numeric band density and background values were acquired using ImageJ software [National Institutes of Health (NIH)]. Mean density values were normalized for each immunoblot by dividing each experimental band density by the mean WT control density.

Western blots of proteins extracted from 3xTg-AD mice were imaged/quantified using a LICOR Odyssey CLx (LI-COR Biosciences) attached to a Dell computer (OptiPlex 7010) running Windows 7 and Image Studio (version 1.0.11, LI-COR Biosciences). Loading controls are provided for all immunoblots shown.

2.4 Antibodies

β-actin (#4967, 1:1000, MW=42kD), AKT (#4056 or #9272, 1:1000, MW=60kD), pAKT (Thr308, #4056, 1:1000), pAKT (Ser473, #4060 or #9271, 1:10000), AMPK (#2603, 1:1000, MW=62kD), pAMPK (Thr172, #2535, 1:500), GSK-3β (#9315, 1:1000, MW=47kD), PDK1 (#3062, 1:1000, MW=63kD), pPDK1 (S241, #4056, 1:1000), IRS-1 (#7200, 1:100, MW=180kD), PI3K p85 (#4292, 1:1000, MW=85kD), pPI3K (p85 Tyr485, #4228, MW= 60-85kD), ERK 1/2 (#9102, 1:1000, MW=44/42kD) were from Cell signaling; pIRS-1 (Ser612, #44-550G, 1:500) was from Invitrogen. pGSK-3β (Tyr216, #05-413, 1:1000) was from Upstate (Millipore).

2.5 Statistical analyses

Data are reported as mean +/− SEM. Outliers were defined as exhibiting a mean ≥ two standard deviations from the mean of the group. Repeated measures ANOVAs were used to analyze the glucose tolerance data. Student's unpaired t-test was employed for pairwise comparison between WT and transgenic mice within each age sampled as we utilized a cross-sectional design. Significance was set to $p \leq 0.05$.

3. Results

3.1 Age-dependent onset of peripheral insulin resistance

Tg2576 mice develop age-dependent peripheral insulin resistance as demonstrated by altered glucose tolerance test (Rodriguez-Rivera et al., 2011; Table 1). To assess changes in peripheral glucose metabolism in 3xTg-AD mice, we performed a glucose tolerance test in 10- and 16-month-old 3xTg-AD and age-matched wildtype (WT) mice. At both of these ages, 3xTg-AD mice show cognitive deficits, while they have established extracellular plaques at 16 but not at 10 months of age (Oddo et al., 2008). We found that fasting glucose levels at 10 months of age were not significantly different between WT and 3xTg-AD mice (101.12 +/− 7.28 mg/dL for WT and 105.45 +/− 9.01 mg/dL for 3xTg-AD mice); at this age, the ability of 3xTg-AD mice to restore their glucose levels back to baseline after a bolus of glucose injected i.p. (time 0 min) was not significantly different compared to WT mice (Table 1 and Fig. 1A). In contrast, 16-month-old 3xTg-AD mice had significantly elevated fasting glucose levels (132.154 +/− 5.578 mg/dL) compared to WT mice (82.727 +/− 3.38 mg/dL) and displayed impairments in their ability to restore the elevated glucose levels during the glucose tolerance test (Fig. 1B). Specifically, glucose levels in 3xTg-AD mice were significantly higher than WT mice at 15, 60, 90 and 120 minutes after the injection of 2 mg/kg bolus of glucose. The area under the curve (AUC) of a glucose tolerance test provides a better assessment of glucose tolerance. AUC analysis indicated that glucose tolerance was not different between 10-month-old 3xTg-AD and WT mice (Fig. 1C). However, at 16 months of age, AUC was significantly higher in 3xTg-AD than WT mice (Fig. 1C). Taken together, these data suggest peripheral glucose insulin resistance in 16-month-old 3xTg-AD mice; this finding is consistent with previous reports (Vandal et al., 2015).

Peripheral insulin resistance is often associated with increased body weight and obesity (Kahn et al., 2006). We therefore measured the body weight of 3xTg-AD and WT mice and found that 10- and 16-month-old 3xTg-AD mice weighed significantly more than WT mice

(Fig. 1D). This finding is consistent with previous reports and suggest that weight may be a contributing factor to peripheral insulin resistance observed in 3xTg-AD mice (Kahn et al., 2006; Knight et al., 2013).

3.2 Age-dependent dysregulation of CNS insulin signaling

Given that both Tg2576 and 3xTg-AD mice develop peripheral insulin resistance, we measured components of the CNS insulin signaling pathway to determine whether brain insulin signaling is dysregulated. Specifically, we measured both total and phosphorylated levels of receptor substrate 1 (IRS-1) and key mediators of IRS coupling, phosphoinositide 3-kinases (PI3K), phosphoinositide-dependent kinase-1 (PDK1), alpha serine/threonine-protein kinase (AKT), and glycogen synthase kinase-3 (GSK3-β). We focused on these proteins because their dysregulation through hypo- and hyper-phosphorylation are implicated in central insulin resistance (Gual et al., 2005; Pederson et al., 2001; Steen et al., 2005; Tanti and Jager, 2009). Briefly, insulin binds to the insulin receptor (IR), which in turn activates IRS-1, whose activity in the brain is necessary for synaptic plasticity and memory consolidation (Horwood et al., 2006). IRS-1 can then activate PI3K, which is required for a wide variety of cellular responses downstream of insulin (Alessi and Downes, 1998). Specifically, phosphorylated IRS recruits the heterodimeric p85/p110 PI3K at the plasma membrane, where it produces the second messenger phosphatidylinositol-4,5-bisphosphate 3- (PIP3) kinase, which in turn activates a serine/threonine phosphorylation cascade of PH-domain containing proteins (Alessi and Downes, 1998). PIP3 targets include PDK1, the serine/threonine protein kinase B (PKB)/Akt, and the atypical protein kinases C ζ and λ isoforms (Dineley et al., 2014; Vandal et al., 2015). GSK-3β, a convergent target of the PDK1/AKT pathways, induces glycogen synthesis through the target of rapamycin complexes to control AMP-activated protein kinase (AMPK), energy metabolism, mitochondrial function, synaptic plasticity and memory (Cheng et al., 2010; Kleinridders et al., 2014; Stoica et al., 2011; White, 2003). Notably, these proteins contribute to insulin resistance through feedback inhibition of IRS (Boura-Halfon and Zick, 2009a; Gual et al., 2005). This provides a variety of pathways that may compromise insulin signaling and subsequently insulin resistance.

Here, we used: 5- and 9-month-old Tg2576 mice. At 5 months of age these mice are yet to develop extracellular Aβ plaques, while numerous plaques are readily detected at 9 months of age (Ashe, 2006). We also used 3xTg-AD mice at 10 months of age, prior to the development of extracellular Aβ plaques, and at 16 months of age, when Aβ plaques are numerous and present throughout the hippocampus and cortex (Oddo et al., 2003). We found that, in 5-month-old Tg2576 mice, total IRS-1 levels were similar to those of WT mice; however, at 9 months of age, after plaques are readily detected in the brain of Tg2576 mice, IRS-1 levels were reduced compared to age-matched WT mice (Fig. 2A, B). We next examined IRS-1 levels phosphorylated at Ser612, as increased phosphorylation at this epitope reduces IRS-1 activity and positively correlates with amyloid oligomers and memory deficits in MCI and AD (Talbot et al., 2012a). The levels of IRS-1 phosphorylated at Ser612 were unaltered in 5-month-old Tg2576 compared to age-matched WT mice (Fig. 2C). In contrast, these levels were higher in 9-month-old Tg2576 mice compared to WT, providing a clear indication of reduced IRS-1 activity and CNS insulin dysregulation.

In 3xTg-AD mice, we found that total IRS-1 levels were reduced compared to WT mice at 10 months of age, before the onset of plaque deposition (Fig. 2D, E). Paradoxically, in 16-month-old 3xTg-AD mice with established Aβ plaques, IRS-1 levels were significantly higher than WT mice (Fig. 2D, E). However, the levels of IRS-1 phosphorylated at Ser612 were significantly reduced in 10-month-old but not in 16-month-old 3xTg-AD mice (Fig. 2D, F). The decrease phosphorylation of IRS-1 at Ser612 at 10 months could indicate a compensatory mechanism to reduce inhibition since IRS-1 total levels are already reduced in these mice. The elevation in total IRS-1 levels in 16-month-old 3xTg-AD mice may be a result of structural brain changes accompanied by AD-pathology. Collectively, these results illustrate dysregulated IRS-1 activity in both mouse models of AD.

To further assess the effects of dysregulated IRS-1 activity on downstream insulin signaling targets, we next measured total PI3K p85 and phosphorylated levels of pPI3K p85 at Tyr458. Both 5- and 9-month-old Tg2576 mice show equal levels of total PI3K p85 activity (Figure 3A, B). In contrast, 9-month-old Tg2576 mice, but not 5-month-old mice, show a significantly elevated level of pPI3K p85 at Tyr458 compared to age-matched WT mice (Figure 3A, C). These results provide a clear indication of increased PI3K activity, which is consistent with changes in IRS-1 levels and illustrate CNS insulin dysregulation.

In 3xTg-AD mice, we found no significant differences in total PI3K p85 levels in 10- and 16-month-old mice (Figure 3D, E). Consistent with IRS-1 activity, we found that levels of pPI3K p85 at Tyr458 are significantly reduced in both 10- and 16-month-old 3xTg-AD mice compared to age-matched WT mice (Figure 3D, F). This is consistent with dysregulation of IRS-1 activity before the onset of peripheral insulin resistance in 3xTg-AD mice and illustrates that CNS insulin resistance preceding peripheral insulin resistance.

To further assess insulin signaling in Tg2576 and 3xTg-AD mice, we measured total and phosphorylated levels of PDK1, which is phosphorylated by PI3K. Specifically, in 5-month-old Tg2576 mice, but not in 9-month-old mice, the levels of total PDK1 protein were significantly increased compared to age-matched WT mice (Fig. 4A, B). Phosphorylation of PDK1 at Ser241 (pPDK1) activates the catalytic function of this enzyme (Casamayor et al., 1999). We found that pPDK1 levels were significantly increased in 5-month-old Tg2576 mice compared to age-matched WT mice (Fig. 4A, C). In contrast, in 9-month-old Tg2576 mice, the levels of pPDK1 were significantly decreased compared to age-matched WT mice. These results suggest that the activity of PDK1 is dysregulated early before the onset of peripheral insulin resistance. Additionally, PDK1 activity becomes reduced consistent with the age when Aβ pathology is apparent in Tg2576 mice.

In 3xTg-AD mice, we found no significant differences in total PDK1 levels at 10 months of age compared to WT mice. However, we found a significantly reduced level at 16 months of age (Fig. 4D, E). Additionally, we found a significantly reduced level of pPDK1 in 10-month-old 3xTg-AD mice compared to age-matched WT mice (Fig. 4D, F). A similar pattern was observed in 16-month-old 3xTg-AD mice. However, this difference failed to reach statistical significance. Taken together, these data suggest that PDK1 activity is dysregulated prior to the onset of peripheral insulin resistance in both Tg2576 and 3xTg-AD mice.

We next measured total and phosphorylated AKT levels as AKT is an integral component of the insulin signaling pathway. Total levels of AKT remained unchanged for both 5- and 9-month-old Tg2576 mice relative to age-matched WT mice (Fig. 5A, B). We therefore examined the levels of AKT phosphorylated (pAKT) at Thr308 and Ser473, as phosphorylation of these epitopes leads to full activation of AKT (Hanada et al., 2004). Five-month-old Tg2576 mice show no significant differences in pAKT at Thr308 and Ser473 relative to age-matched WT (Fig. 5A, C). However, we found a significant reduction of pAKT Thr308 and a significant increase of pAKT Ser473 in 9-month-old Tg2576 mice relative to age-matched WT mice. (Fig. 5A, D). The increase in pAKT activity in 9-month-old Tg2576 mice may be a result of alterations of alternative pathways associated with Aβ pathology (Hanada et al., 2004).

In 3xTg-AD mice, we found that the total levels of AKT remained unchanged at both ages analyzed (Fig. 5E, F). Similarly, 10-month-old 3xTg-AD mice show no significant differences compared to age-matched WT mice for pAKT Thr308 and pAKT Ser473 levels. In contrast, we found that the levels of pAKT phosphorylated at these two epitopes were significantly increased in 16-month-old 3xTg-AD mice compared to their age-matched WT mice (Fig. 5E, G–H). Similar to Tg2576 mice, the increase in pAKT activity in 16-month-old 3xTg-AD mice may be a result of alterations of alternative pathways associated with Aβ pathology (Hanada et al., 2004).

GSK-3β is a convergent target of the PDK1/AKT pathways as well as a key negative regulator of IRS-1 (Henriksen and Dokken, 2006; Talbot et al., 2012a). We found that the total levels of GSK-3β remained unchanged in 5- and 9-month-old Tg2576 mice relative to WT mice (Fig. 6A, B). GSK-3β activity is regulated by phosphorylation of Tyr216 (pGSK-3β), which is necessary for its activity (Bhat et al., 2000). We found that pGSK3β at Tyr216 was similar between 5-month-old Tg2576 and WT mice (Fig. 6A, C). There was however a significantly elevated level in 9-month-old Tg2576 mice relative to WT mice. These results suggest that prior to the onset of peripheral insulin resistance, GSK-3β activity is unaltered in Tg2576 mice relative to WT mice. The activity of GSK-3β then increases after the onset of peripheral insulin resistance.

For the 3xTg-AD mice, we found that the total levels of GSK-3β remained unchanged in 10- and 16-month-old mice relative to age-matched WT mice (Fig. 6D, E). Similar to Tg2576 mice, we found that the levels of pGSK-3β at Tyr216 were not significantly different between 10-month-old 3xTg-AD and WT mice, but they were significantly elevated level in 16-month-old 3xTg-AD mice relative to WT mice (Fig. 6D, H). These results are consistent with GSK-3β activity in Tg2576 mice and suggest an age-dependent increase in GSK-3β consecutive to the onset of peripheral insulin resistance. Collectively, these results show that both animal models of AD exhibit dysregulation of the various components of the *central* insulin signaling pathway months prior to the onset of *peripheral* insulin resistance.

3.3 Age-dependent dysregulation of phosphorylated AMPK levels in Tg2576 and 3xTg-AD mice

Cognitive impairments associated with diabetes and AD include a process beyond insulin resistance and encompass energy homeostasis (Denner et al., 2012; Kobilo et al., 2014;

Rodriguez-Rivera et al., 2011; Saha et al., 2010). AMPK is a key sensor of energy homeostasis and is activated when energy levels are diminished (Kobilo et al., 2014). We thus evaluated the activity of AMPK in Tg2576 and 3xTg-AD mice as a function of age. Notably, we included a Tg2576 13-month-old age group to determine whether AMPKs activity changes when Aβ accumulation is further progressed (Ashe, 2006). We found that compared to WT mice, AMPK levels in Tg2576 mice were increased at 13 months of age but not at 9 months of age (Fig. 7A, B). We next measured the phosphorylated levels of AMPK (pAMPK) at Thr172 as phosphorylation of this epitope increases the activity of AMPK (Hawley et al., 1996). We found that 9-month-old Tg2576 mice show no difference relative to age-matched WT mice, however there was a significant reduction in 13-month-old Tg2576 mice relative to their age-match WT mice (Fig. 7A, C). These results suggest that metabolic energy homeostasis is altered in Tg2576 mice at an age well beyond the onset of central insulin dysregulation and Aβ accumulation.

In 3xTg-AD mice, we found that the levels of AMPK were not statistically different compared to WT mice at both ages analyzed (Fig. 7D–E). In contrast, we found that pAMPK levels at Thr172 were increased in 10- but not in 16-month-old 3xTg-AD mice compared to age-matched WT mice (Fig. 7D, F). These results suggest that 3xTg-AD mice exhibit altered pAMPK Thr172 levels coincident with central insulin dysregulation (10 months of age).

4. DISCUSSION

Type 2 diabetes (T2D) and Alzheimer's disease (AD) are two of the most prominent diseases plaguing the aging population (Alzheimer's Association, 2016; Baglietto-Vargas et al., 2016; Zilliox et al., 2016). Epidemiological, clinical, and preclinical, evidence compellingly suggests that T2D and AD bear interrelated disease risks and mechanisms (Haan, 2006; Heneka et al., 2015; Janson et al., 2004; Kandimalla et al., 2016; Steen et al., 2005). However, significant gaps in knowledge still exist concerning the relationship between CNS and peripheral insulin signaling with cognitive function and AD pathology. Our results show that in two mouse models of AD-like pathology, central insulin signaling markers are dysregulated prior to the onset of peripheral insulin resistance and central insulin resistance occurs concomitant with manifestation of AD-like cognitive deficits and oligomeric amyloid pathology (Park, 2011; Talbot et al., 2012; Zhang et al., 2012). Furthermore, we have evidence that tau pathology contributes to more severe CNS insulin resistance in 3xTg-AD mice.

Again, since both models are genetically programmed to overproduce Aβ and exhibit AD-like amyloidosis suggests that this amyloid pathology is a primary driver of central and peripheral insulin resistance and downstream effects on effectors of energy homeostasis (e.g., AMPK). Since, tau pathology is often observed in models of insulin resistance, T2D, and AD, the additional phenotype of tau pathology in 3xTg-AD mice is a candidate explanation for the general observation of more extensive dysregulation of CNS insulin signaling intermediaries observed in 3xTg-AD compared to Tg2576 mice (Baglietto-Vargas et al., 2016; Ke et al., 2009; Kim et al., 2013; Qi et al., 2016; Yarchoan et al., 2014). Future

studies directed at the specific effects of tau in CNS insulin signaling will elucidate this relationship.

Peripheral insulin resistance is commonly evaluated with the GTT by measuring blood glucose clearance after a bolus intravenous injection of glucose with fasting. Using the GTT on our two mouse models, we found that glucose metabolism is normal in 3xTg-AD mice at 10 months of age but deficient by 16 months of age, as evidenced by a marked delay in blood glucose clearance. This is consistent with our previous work showing that peripheral glucose metabolism is affected in Tg2576 mice at 9 and 13 months of age but not at 5 months of age when cognitive deficits first manifest (Rodriguez-Rivera et al., 2011). The correlation between the age-of-onset of peripheral GTT deficits with Aβ oligomer pathology and cognitive deficits are notably consistent between these two AD mouse models (Ashe, 2006; Oddo et al., 2008). In support, a recent publication using 3xTg-AD mice reported that peripheral glucose intolerance and cortical Aβ deposition progressively worsened from 10 and 14 months of age (Vandal et al., 2015). Furthermore, the weight of 3xTg-AD mice was significantly elevated at both 10 and 16 months of age, while peripheral insulin resistance was not observed until 16 months of age, suggesting that weight is not the only factor leading to impaired peripheral glucose insulin resistance in 3xTg-AD mice. Collectively, these results suggest that peripheral insulin resistance manifests in Tg2576 and 3xTg-AD mice after the initiation of cognitive and central insulin signaling deficits.

A well-established, albeit not exclusive, biomarker of insulin resistance is phosphorylation (hyper- and hypo-phosphorylation) of IRS-1 at serine residues (Boura-Halfon and Zick, 2009a; Gual et al., 2005; Pederson et al., 2001; Sun and Liu, 2009; Talbot et al., 2012; Zhang et al., 2016). IRS-1 serine phosphorylation results from feedback inhibition exerted mainly by ERK2, GSK-3β, mTOR and atypical protein kinase C (PKCζ/λ) and from feed-forward inhibition exerted by nuclear factor NF-κB and c-Jun N-terminal kinases (JNK ½) (Boura-Halfon and Zick, 2009a, 2009b; Gual et al., 2005; Sun and Liu, 2009; Tanti and Jager, 2009). To this end, both *in vitro* and *in vivo* work has shown that Aβ can induce insulin resistance by activating the Janus kinase 2 (JAK2)/Signal transducer and activator of transcription 3 (STAT3)/Suppressor of cytosine signaling 1 (SOCS-1) signaling pathway (Zhang et al., 2013, 2012). Thus, we looked at the downstream IRβ substrate IRS-1 Ser612 phosphorylation, which correlates with amyloid oligomers and memory in MCI and AD (Talbot et al., 2012). 9-month-old Tg2576 mice exhibited hippocampal Ser612 hyper-phosphorylation of the IRS-1 protein. These data are consistent with previous work showing IRS-1 Ser612 hyper-phosphorylation in APP/PS1 transgenic mice of a similar age (Long-Smith et al., 2013). Regarding 3xTg-AD mice, we found evidence for CNS insulin resistance in 10-month-old mice as indicate by reduced total and Ser612 phopho-IRS-1. These markers continue to be dysregulated at 16 months of age when peripheral insulin resistance is detectable with the GTT. Similar to Tg2576, CNS insulin resistance in 10-month-old 3xTg-AD mice coincides with the onset of hippocampal-dependent cognitive deficits (Oddo et al., 2003; Vandal et al., 2015). Thus, as is the case in MCI and AD subjects, brain insulin resistance appears to be an early and common feature in two animal models for amyloidosis and precedes peripheral insulin resistance. In support of our hypothesis that central insulin resistance is intermingled with AD-like pathology and cognitive decline in Tg2576 and 3xTg-AD mice, we found that the total and phosphorylation levels of PI3K, PDK1, and

AKT changed as a function of age that simulate a chain reaction of the insulin signaling cascade. For instance, PI3K phosphorylation is consistent with altered PDK1 phosphorylation levels, as PDK1 is a target of PI3K and decreased pAKT at Thr308 is internally consistent since the latter is a PDK1 target. Furthermore, elevated levels of pAKT at Thr308 and Ser473 in 3xTg-AD mice at 16 months of age are internally consistent with the upstream observations of PDK1. It should be noted that these changes are consistent with results in Tg2576 mice. Notably, the increases in AKT phosphorylation seen in 3xTg-AD mice do not appear to be driven by obesity as the body weight of 3xTg-AD mice was significantly higher than age-matched WT mice at both age groups analyzed, whereas AKT activity is increased only at 16 months of age. Alteration of AKT signaling has emerged as an important feature of neurodegenerative diseases characterized by neuronal attrition, which includes AD (Griffin et al., 2005). Our results on the effects of AKT activity are consistent with this feature as dysregulation was evident after the onset of Aβ pathology.

GSK-3β is a convergent target of the PDK1/AKT and ERK MAPK pathways as well as a key negative regulator of IRS-1 (Talbot et al., 2012). AKT drives GLUT (glucose transporter) plasma membrane translocation to normalize blood glucose and activates GSK-3β to induce glycogen synthesis through the target of rapamycin complexes, including mTOR, to control AMPK, energy metabolism, mitochondrial function, synaptic plasticity and memory (Cheng et al., 2010; Kleinridders et al., 2014; Stoica et al., 2011). GSK-3β activity is increased by phosphorylation of Tyr216 (Bhat et al., 2000). At 9 months of age, pGSK-3β at Tyr216 is elevated in Tg2576, suggesting that GSK-3β is enhanced at this age by AKT and potentially through other signaling pathways. To this end, GSK-3β can be phosphorylated by pAKT at Thr308, and is also targeted by protein kinase A, protein kinase B, protein kinase C-ζ, and p90 ribosomal S6 kinase, indicating that these GSK-3β alterations may additionally occur independent of the IR-IRS-PI3K-PDK1-AKT signaling pathway (Medina and Wandosell, 2011). Interestingly, these same patterns were seen in the 3xTg-AD mice in which we found elevated levels of pGSK-3β at Try216 at 16 months of age, consistent with peripheral insulin resistance and increased AKT activity. To this end, researchers have shown that the GSK-3 pathway, when dysregulated by insulin resistance, facilitates the Aβ plaques pathology (Phiel et al., 2003) and is linked to tau misfolding and toxicity (Bosco et al., 2011; Himmelstein et al., 2012; Luchsinger, 2010).

It must be noted that the baseline status of CNS insulin signaling intermediaries was divergent between the two mouse models analyzed here. Specifically, while both mouse models exhibit significant dysregulation of PDK1 activity before the onset of peripheral insulin resistance, 3xTg-AD mice exhibit a much more aggressive CNS insulin resistance phenotype. For instance, IRS-1 and PI3K phosphorylation were significantly reduced in 3xTg-AD mice prior to the onset of peripheral insulin resistance whereas Tg2576 mice show dysregulation of these markers after the onset of peripheral insulin resistance. These discrepancies may be specific to the tau pathology that develops in 3xTg-AD mice. It is well established that tau protein is regulated by insulin and IGF signaling and insulin signaling dysregulation often results in tau (de la Monte, 2012; Himmelstein et al., 2012; Ke et al., 2009; Yarchoan et al., 2014). Thus, it is likely that the more robust changes in insulin signaling in older 3xTg-AD mice leads to tau hyperphosphorylation, possibly through

altered function of tau kinases and phosphatases (de la Monte, 2012; Ke et al., 2009; Mairet-Coello et al., 2013; Mullins et al., 2017; Vingtdeux et al., 2011).

Energy homeostasis is an additional dimension to the cellular and physiological dysfunction related to insulin resistance and T2D (Carling, 2017; Porte, 2006; Saha et al., 2010). AMPK is a key cellular sensor of energy reserves and a significant diabetes therapeutic target to increase insulin sensitivity (Misra, 2008; Misra and Chakrabarti, 2007; Musi, 2006). In the CNS, AMPK has been shown to have important, but complex, roles in energy balance (Kobilo et al., 2014). AMPK is dysregulated concomitant with central insulin resistance in 10-month-old 3xTg-AD mice yet occurs much later in 13-month-old Tg2576 mice and is associated with further decline in Tg2576 mice cognitive function (Ashe, 2006; Cacucci et al., 2008; Dineley et al., 2001; Kotilinek et al., 2002; Saha et al., 2010; Westerman et al., 2002). Paradoxically, we found that AMPK activity (i.e., pAMPK at Thr172 levels) was increased in 10-month-old 3xTg-AD brain. To this end, studies increased AMPK activity upregulates tau phosphorylation (Mairet-Coello et al., 2013; Thornton et al., 2011; Vingtdeux et al., 2011). Further, Mariet-Coello and colleagues found that $A\beta_{42}$ oligomers trigger activation of AMPK which in turn promote the phosphorylation of tau (Mairet-Coello et al., 2013). Furthermore, it has been demonstrated that recombinant AMPK phosphorylates tau protein at numerous sites in the microtubule-binding domain and within the flanking regions (Thornton et al., 2011; Vingtdeux et al., 2011). Given that the 3xTg-AD mice develop NFTs, this suggests that AMPK upregulation may contribute to or even be a consequence of the tau pathology unique to this model (Oddo et al., 2003). Additionally, AD is associated with multi-dimensional abnormalities in energy metabolism, for example, mitochondrial dysfunctions, decline in glucose uptake, and defects in cholesterol metabolism and Ca^{2+} homeostasis (Galindo et al., 2010; LaFerla, 2002; Martins et al., 2009; Mosconi et al., 2008). Considering the capability of AMPK to influence these mechanisms, the observed defects in AMPK in 3xTg-AD and Tg2576 mice that coincide with the progression of insulin resistance are a compelling subject for future investigation.

5. CONCLUSIONS

Our data suggest an age-dependent progression of CNS insulin signaling dysregulation that precedes peripheral insulin resistance in two preclinical models of AD. Importantly, these CNS insulin signaling abnormalities are more apparent in 3xTg-AD mice, which develop Aβ and tau pathology. Interestingly, the respective age-dependent onset of dysfunctional central insulin signaling coincides with the onset of cognitive impairment described for these two preclinical models of AD. These results suggest that early AD may reflect engagement of different signaling networks that influence CNS metabolism, which in-turn alter peripheral insulin signaling. Additionally, our data show that energy metabolism is dysregulated both pre- and post-peripheral insulin resistance and its dysregulation may be specific to Aβ and tau pathology in our preclinical AD models. Peripheral insulin resistance may further contribute to brain pathology and functional abnormalities in AD, creating a vicious cycle which further augments AD-neuropathology. Collectively, this work suggests that reducing CNS insulin signaling dysfunction in patients with MCI or early stage AD may help reduce peripheral insulin resistance, possibly deterring this insidious cycle.

Acknowledgments

This work was supported by the National Institutes of Health under R01-AG031859 to KTD and LD and by the National Institute on Aging R01-AG037637 to SO. Additional funding was provided by the Bright Focus Foundation, Alzheimer's Association, and The Sealy Foundation for Biomedical Research to KTD; by the Miriam and Emmett McCoy Foundation to LD; a kind gift from J and W Mohn to KTD and LD, and by the Cullen Trust for Health Care to the Mitchell Center.

Abbreviations

Aβ	amyloid-β peptide
AD	Alzheimer's disease
AKT	alpha serine/threonine-protein kinase
AMPK	AMP-activated kinase
CNS	central nervous system
CTRL	control
GSK-3β	glycogen synthase kinase 3 beta
GTT	glucose tolerance test
IR	insulin receptor
IRS	insulin receptor substrate
MCI	mild cognitive impairment
mTOR	mammalian target of rapamycin
PDK1	phosphoinositide-dependent kinase1
PGC-1	PPARγ co-activator 1 alpha
WT	wild type

References

Alessi DR, Downes CP. The role of PI 3-kinase in insulin action. Biochim Biophys Acta. 1998; 1436:151–164. [PubMed: 9838087]

Alex, ADA. [accessed 10.3.16] Statistics About Diabetes [WWW Document]. Am Diabetes Assoc. n.d. 1701 N.B.S., ria, 1-800-Diabetes, V. 22311URL http://www.diabetes.org/diabetes-basics/statistics/

Alzheimer's, Association. 2016 Alzheimer's disease facts and figures. Alzheimers Dement J Alzheimers Assoc. 2016; 12:459–509.

Ashe KH. Molecular basis of memory loss in the Tg2576 mouse model of Alzheimer's disease. J Alzheimers Dis JAD. 2006; 9:123–126. [PubMed: 16914850]

Baglietto-Vargas D, Shi J, Yaeger DM, Ager R, LaFerla FM. Diabetes and Alzheimer's disease crosstalk. Neurosci Biobehav Rev. 2016; 64:272–287. DOI: 10.1016/j.neubiorev.2016.03.005 [PubMed: 26969101]

Bhat RV, Shanley J, Correll MP, Fieles WE, Keith RA, Scott CW, Lee CM. Regulation and localization of tyrosine216 phosphorylation of glycogen synthase kinase-3β in cellular and animal models of neuronal degeneration. Proc Natl Acad Sci U S A. 2000; 97:11074–11079. [PubMed: 10995469]

Bosco D, Fava A, Plastino M, Montalcini T, Pujia A. Possible implications of insulin resistance and glucose metabolism in Alzheimer's disease pathogenesis. J Cell Mol Med. 2011; 15:1807–1821. DOI: 10.1111/j.1582-4934.2011.01318.x [PubMed: 21435176]

Boura-Halfon S, Zick Y. Phosphorylation of IRS proteins, insulin action, and insulin resistance. Am J Physiol Endocrinol Metab. 2009a; 296:E581–591. DOI: 10.1152/ajpendo.90437.2008 [PubMed: 18728222]

Boura-Halfon S, Zick Y. Serine kinases of insulin receptor substrate proteins. Vitam Horm. 2009b; 80:313–349. DOI: 10.1016/S0083-6729(08)00612-2 [PubMed: 19251043]

Caccamo A, Branca C, Talboom JS, Shaw DM, Turner D, Ma L, Messina A, Huang Z, Wu J, Oddo S. Reducing Ribosomal Protein S6 Kinase 1 Expression Improves Spatial Memory and Synaptic Plasticity in a Mouse Model of Alzheimer's Disease. J Neurosci. 2015; 35:14042–14056. DOI: 10.1523/JNEUROSCI.2781-15.2015 [PubMed: 26468204]

Cacucci F, Yi M, Wills TJ, Chapman P, O'Keefe J. Place cell firing correlates with memory deficits and amyloid plaque burden in Tg2576 Alzheimer mouse model. Proc Natl Acad Sci U S A. 2008; 105:7863–7868. DOI: 10.1073/pnas.0802908105 [PubMed: 18505838]

Cao D, Lu H, Lewis TL, Li L. Intake of sucrose-sweetened water induces insulin resistance and exacerbates memory deficits and amyloidosis in a transgenic mouse model of Alzheimer disease. J Biol Chem. 2007; 282:36275–36282. DOI: 10.1074/jbc.M703561200 [PubMed: 17942401]

Carling D. AMPK signalling in health and disease. Curr Opin Cell Biol. 2017; 45:31–37. DOI: 10.1016/j.ceb.2017.01.005 [PubMed: 28232179]

Carvalho C, Cardoso S, Correia SC, Santos RX, Santos MS, Baldeiras I, Oliveira CR, Moreira PI. Metabolic alterations induced by sucrose intake and Alzheimer's disease promote similar brain mitochondrial abnormalities. Diabetes. 2012; 61:1234–1242. DOI: 10.2337/db11-1186 [PubMed: 22427376]

Casamayor A, Morrice NA, Alessi DR. Phosphorylation of Ser-241 is essential for the activity of 3-phosphoinositide-dependent protein kinase-1: identification of five sites of phosphorylation in vivo. Biochem J. 1999; 342:287–292. [PubMed: 10455013]

Cheng Z, Tseng Y, White MF. Insulin signaling meets mitochondria in metabolism. Trends Endocrinol Metab TEM. 2010; 21:589–598. DOI: 10.1016/j.tem.2010.06.005 [PubMed: 20638297]

de la Monte SM. Contributions of brain insulin resistance and deficiency in amyloid-related neurodegeneration in Alzheimer's disease. Drugs. 2012; 72:49–66. DOI: 10.2165/11597760-000000000-00000 [PubMed: 22191795]

Denner LA, Rodriguez-Rivera J, Haidacher SJ, Jahrling JB, Carmical JR, Hernandez CM, Zhao Y, Sadygov RG, Starkey JM, Spratt H, Luxon BA, Wood TG, Dineley KT. Cognitive enhancement with rosiglitazone links the hippocampal PPARγ and ERK MAPK signaling pathways. J Neurosci Off J Soc Neurosci. 2012; 32:16725–16735a. DOI: 10.1523/JNEUROSCI.2153-12.2012

Dineley KT, Jahrling JB, Denner L. Insulin Resistance in Alzheimer's Disease. Neurobiol Dis. 2014; 72PA:92–103. DOI: 10.1016/j.nbd.2014.09.001

Dineley KT, Westerman M, Bui D, Bell K, Ashe KH, Sweatt JD. Beta-amyloid activates the mitogen-activated protein kinase cascade via hippocampal alpha7 nicotinic acetylcholine receptors: In vitro and in vivo mechanisms related to Alzheimer's disease. J Neurosci Off J Soc Neurosci. 2001; 21:4125–4133.

Galbo T, Olsen GS, Quistorff B, Nishimura E. Free fatty acid-induced PP2A hyperactivity selectively impairs hepatic insulin action on glucose metabolism. PloS One. 2011; 6:e27424.doi: 10.1371/journal.pone.0027424 [PubMed: 22087313]

Galbo T, Perry RJ, Nishimura E, Samuel VT, Quistorff B, Shulman GI. PP2A inhibition results in hepatic insulin resistance despite Akt2 activation. Aging. 2013; 5:770–781. DOI: 10.18632/aging.100611 [PubMed: 24150286]

Goldstein ME, Cao Y, Fiedler T, Toyn J, Iben L, Barten DM, Pierdomenico M, Corsa J, Prasad CVC, Olson RE, Li YW, Zaczek R, Albright CF. Ex vivo occupancy of gamma-secretase inhibitors

correlates with brain beta-amyloid peptide reduction in Tg2576 mice. J Pharmacol Exp Ther. 2007; 323:102–108. DOI: 10.1124/jpet.107.125492 [PubMed: 17640949]

Griffin RJ, Moloney A, Kelliher M, Johnston JA, Ravid R, Dockery P, O'Connor R, O'Neill C. Activation of Akt/PKB, increased phosphorylation of Akt substrates and loss and altered distribution of Akt and PTEN are features of Alzheimer's disease pathology. J Neurochem. 2005; 93:105–117. DOI: 10.1111/j.1471-4159.2004.02949.x [PubMed: 15773910]

Grober E, Hall CB, Lipton RB, Zonderman AB, Resnick SM, Kawas C. Memory impairment, executive dysfunction, and intellectual decline in preclinical Alzheimer's disease. J Int Neuropsychol Soc. 2008; :14.doi: 10.1017/S1355617708080302

Gual P, Le Marchand-Brustel Y, Tanti JF. Positive and negative regulation of insulin signaling through IRS-1 phosphorylation. Biochimie. 2005; 87:99–109. DOI: 10.1016/j.biochi.2004.10.019 [PubMed: 15733744]

Haan MN. Therapy Insight: type 2 diabetes mellitus and the risk of late-onset Alzheimer's disease. Nat Rev Neurol. 2006; 2:159–166. DOI: 10.1038/ncpneuro0124

Hanada M, Feng J, Hemmings BA. Structure, regulation and function of PKB/AKT--a major therapeutic target. Biochim Biophys Acta. 2004; 1697:3–16. DOI: 10.1016/j.bbapap.2003.11.009 [PubMed: 15023346]

Hawley SA, Davison M, Woods A, Davies SP, Beri RK, Carling D, Hardie DG. Characterization of the AMP-activated Protein Kinase Kinase from Rat Liver and Identification of Threonine 172 as the Major Site at Which It Phosphorylates AMP-activated Protein Kinase. J Biol Chem. 1996; 271:27879–27887. DOI: 10.1074/jbc.271.44.27879 [PubMed: 8910387]

Head E, Lott IT, Wilcock DM, Lemere CA. Aging in Down syndrome and the Development of Alzheimer's disease Neuropathology. Curr Alzheimer Res. 2016; 13:18. [PubMed: 26651341]

Heneka MT, Fink A, Doblhammer G. Effect of pioglitazone medication on the incidence of dementia. Ann Neurol. 2015; 78:284–294. DOI: 10.1002/ana.24439 [PubMed: 25974006]

Henriksen EJ, Dokken BB. Role of glycogen synthase kinase-3 in insulin resistance and type 2 diabetes. Curr Drug Targets. 2006; 7:1435–1441. [PubMed: 17100583]

Himmelstein DS, Ward SM, Lancia JK, Patterson KR, Binder LI. Tau as a therapeutic target in neurodegenerative disease. Pharmacol Ther. 2012; 136:8–22. DOI: 10.1016/j.pharmthera.2012.07.001 [PubMed: 22790092]

Ho L, Qin W, Pompl PN, Xiang Z, Wang J, Zhao Z, Peng Y, Cambareri G, Rocher A, Mobbs CV, Hof PR, Pasinetti GM. Diet-induced insulin resistance promotes amyloidosis in a transgenic mouse model of Alzheimer's disease. FASEB J Off Publ Fed Am Soc Exp Biol. 2004; 18:902–904. DOI: 10.1096/fj.03-0978fje

Horwood JM, Dufour F, Laroche S, Davis S. Signalling mechanisms mediated by the phosphoinositide 3-kinase/Akt cascade in synaptic plasticity and memory in the rat. Eur J Neurosci. 2006; 23:3375–3384. DOI: 10.1111/j.1460-9568.2006.04859.x [PubMed: 16820027]

Hsiao K, Chapman P, Nilsen S, Eckman C, Harigaya Y, Younkin S, Yang F, Cole G. Correlative memory deficits, Abeta elevation, and amyloid plaques in transgenic mice. Science. 1996; 274:99–102. [PubMed: 8810256]

Jackson SL, Safo SE, Staimez LR, Olson DE, Narayan KMV, Long Q, Lipscomb J, Rhee MK, Wilson PWF, Tomolo AM, Phillips LS. Glucose challenge test screening for prediabetes and early diabetes. Diabet Med J Br Diabet Assoc. 2017; 34:716–724. DOI: 10.1111/dme.13270

Jahrling JB, Hernandez CM, Denner L, Dineley KT. PPARγ recruitment to active ERK during memory consolidation is required for Alzheimer's disease-related cognitive enhancement. J Neurosci Off J Soc Neurosci. 2014; 34:4054–4063. DOI: 10.1523/JNEUROSCI.4024-13.2014

Janson J, Laedtke T, Parisi JE, O'Brien P, Petersen RC, Butler PC. Increased risk of type 2 diabetes in Alzheimer disease. Diabetes. 2004; 53:474–481. [PubMed: 14747300]

Kahn SE, Hull RL, Utzschneider KM. Mechanisms linking obesity to insulin resistance and type 2 diabetes. Nature. 2006; 444:840–846. DOI: 10.1038/nature05482 [PubMed: 17167471]

Kandimalla R, Thirumala V, Reddy PH. Is Alzheimer's disease a Type 3 Diabetes? A critical appraisal. Biochim Biophys Acta BBA - Mol Basis Dis. n.d; doi: 10.1016/j.bbadis.2016.08.018

Ke YD, Delerue F, Gladbach A, Götz J, Ittner LM. Experimental diabetes mellitus exacerbates tau pathology in a transgenic mouse model of Alzheimer's disease. PloS One. 2009; 4:e7917.doi: 10.1371/journal.pone.0007917 [PubMed: 19936237]

Kim B, Backus C, Oh S, Feldman EL. Hyperglycemia-induced tau cleavage in vitro and in vivo: a possible link between diabetes and Alzheimer's disease. J Alzheimers Dis JAD. 2013; 34:727–739. DOI: 10.3233/JAD-121669 [PubMed: 23254634]

Kivipelto M, Helkala EL, Laakso MP, Hänninen T, Hallikainen M, Alhainen K, Iivonen S, Mannermaa A, Tuomilehto J, Nissinen A, Soininen H. Apolipoprotein E epsilon4 allele, elevated midlife total cholesterol level, and high midlife systolic blood pressure are independent risk factors for late-life Alzheimer disease. Ann Intern Med. 2002; 137:149–155. [PubMed: 12160362]

Kleinridders A, Ferris HA, Cai W, Kahn CR. Insulin action in brain regulates systemic metabolism and brain function. Diabetes. 2014; 63:2232–2243. DOI: 10.2337/db14-0568 [PubMed: 24931034]

Knight EM, Brown TM, Gümüsgöz S, Smith JCM, Waters EJ, Allan SM, Lawrence CB. Age-related changes in core body temperature and activity in triple-transgenic Alzheimer's disease (3xTgAD) mice. Dis Model Mech. 2013; 6:160–170. DOI: 10.1242/dmm.010173 [PubMed: 22864021]

Kobilo T, Guerrieri D, Zhang Y, Collica SC, Becker KG, van Praag H. AMPK agonist AICAR improves cognition and motor coordination in young and aged mice. Learn Mem. 2014; 21:119–126. DOI: 10.1101/lm.033332.113 [PubMed: 24443745]

Kotilinek LA, Bacskai B, Westerman M, Kawarabayashi T, Younkin L, Hyman BT, Younkin S, Ashe KH. Reversible memory loss in a mouse transgenic model of Alzheimer's disease. J Neurosci Off J Soc Neurosci. 2002; 22:6331–6335. 20026675.

LaFerla FM, Oddo S. Alzheimer's disease: Abeta, tau and synaptic dysfunction. Trends Mol Med. 2005; 11:170–176. DOI: 10.1016/j.molmed.2005.02.009 [PubMed: 15823755]

Long-Smith CM, Manning S, McClean PL, Coakley MF, O'Halloran DJ, Holscher C, O'Neill C. The diabetes drug liraglutide ameliorates aberrant insulin receptor localisation and signalling in parallel with decreasing both amyloid-β plaque and glial pathology in a mouse model of Alzheimer's disease. Neuromolecular Med. 2013; 15:102–114. DOI: 10.1007/s12017-012-8199-5 [PubMed: 23011726]

Luchsinger JA. Diabetes, related conditions, and dementia. J Neurol Sci. 2010; 299:35–38. DOI: 10.1016/j.jns.2010.08.063 [PubMed: 20888602]

Mairet-Coello G, Courchet J, Pieraut S, Courchet V, Maximov A, Polleux F. The CAMKK2-AMPK kinase pathway mediates the synaptotoxic effects of Aβ oligomers through Tau phosphorylation. Neuron. 2013; 78:94–108. DOI: 10.1016/j.neuron.2013.02.003 [PubMed: 23583109]

Medina M, Wandosell F. Deconstructing GSK-3: The Fine Regulation of Its Activity. Int J Alzheimers Dis. 2011; 2011:479249.doi: 10.4061/2011/479249 [PubMed: 21629747]

Misra P. AMP activated protein kinase: a next generation target for total metabolic control. Expert Opin Ther Targets. 2008; 12:91–100. DOI: 10.1517/14728222.12.1.91 [PubMed: 18076373]

Misra P, Chakrabarti R. The role of AMP kinase in diabetes. Indian J Med Res. 2007; 125:389–398. [PubMed: 17496363]

Moll L, El-Ami T, Cohen E. Selective manipulation of aging: a novel strategy for the treatment of neurodegenerative disorders. Swiss Med Wkly. 2014; 144:w13917.doi: 10.4414/smw.2014.13917 [PubMed: 24526357]

Mullins RJ, Diehl TC, Chia CW, Kapogiannis D. Insulin Resistance as a Link between Amyloid-Beta and Tau Pathologies in Alzheimer's Disease. Front Aging Neurosci. 2017; 9:118.doi: 10.3389/fnagi.2017.00118 [PubMed: 28515688]

Musi N. AMP-activated protein kinase and type 2 diabetes. Curr Med Chem. 2006; 13:583–589. [PubMed: 16515522]

Oddo S, Caccamo A, Kitazawa M, Tseng BP, LaFerla FM. Amyloid deposition precedes tangle formation in a triple transgenic model of Alzheimer's disease. Neurobiol Aging. 2003; 24:1063–1070. [PubMed: 14643377]

Oddo S, Caccamo A, Tseng B, Cheng D, Vasilevko V, Cribbs DH, LaFerla FM. Blocking Abeta42 accumulation delays the onset and progression of tau pathology via the C terminus of heat shock protein70-interacting protein: a mechanistic link between Abeta and tau pathology. J Neurosci Off J Soc Neurosci. 2008; 28:12163–12175. DOI: 10.1523/JNEUROSCI.2464-08.2008

Orr ME, Salinas A, Buffenstein R, Oddo S. Mammalian target of rapamycin hyperactivity mediates the detrimental effects of a high sucrose diet on Alzheimer's disease pathology. Neurobiol Aging. 2014; 35:1233–1242. DOI: 10.1016/j.neurobiolaging.2013.12.006 [PubMed: 24411482]

Park SA. A common pathogenic mechanism linking type-2 diabetes and Alzheimer's disease: evidence from animal models. J Clin Neurol Seoul Korea. 2011; 7:10–18. DOI: 10.3988/jcn.2011.7.1.10

Pedersen WA, Flynn ER. Insulin resistance contributes to aberrant stress responses in the Tg2576 mouse model of Alzheimer's disease. Neurobiol Dis. 2004; 17:500–506. DOI: 10.1016/j.nbd.2004.08.003 [PubMed: 15571985]

Pederson TM, Kramer DL, Rondinone CM. Serine/Threonine Phosphorylation of IRS-1 Triggers Its Degradation. Diabetes. 2001; 50:24–31. DOI: 10.2337/diabetes.50.1.24 [PubMed: 11147790]

Phiel CJ, Wilson CA, Lee VMY, Klein PS. GSK-3alpha regulates production of Alzheimer's disease amyloid-beta peptides. Nature. 2003; 423:435–439. DOI: 10.1038/nature01640 [PubMed: 12761548]

Porte D. Central Regulation of Energy Homeostasis. Diabetes. 2006; 55:S155–S160. DOI: 10.2337/db06-S019

Qi L, Ke L, Liu X, Liao L, Ke S, Liu X, Wang Y, Lin X, Zhou Y, Wu L, Chen Z, Liu L. Subcutaneous administration of liraglutide ameliorates learning and memory impairment by modulating tau hyperphosphorylation via the glycogen synthase kinase-3β pathway in an amyloid β protein induced alzheimer disease mouse model. Eur J Pharmacol. 2016; 783:23–32. DOI: 10.1016/j.ejphar.2016.04.052 [PubMed: 27131827]

Querfurth HW, LaFerla FM. Alzheimer's disease. N Engl J Med. 2010; 362:329–344. DOI: 10.1056/NEJMra0909142 [PubMed: 20107219]

Ramos-Rodriguez JJ, Spires-Jones T, Pooler AM, Lechuga-Sancho AM, Bacskai BJ, Garcia-Alloza M. Progressive Neuronal Pathology and Synaptic Loss Induced by Prediabetes and Type 2 Diabetes in a Mouse Model of Alzheimer's Disease. Mol Neurobiol. 2016; doi: 10.1007/s12035-016-9921-3

Rodriguez-Rivera J, Denner L, Dineley KT. Rosiglitazone reversal of Tg2576 cognitive deficits is independent of peripheral gluco-regulatory status. Behav Brain Res. 2011; 216:255–261. DOI: 10.1016/j.bbr.2010.08.002 [PubMed: 20709114]

Saedi E, Gheini MR, Faiz F, Arami MA. Diabetes mellitus and cognitive impairments. World J Diabetes. 2016; 7:412–422. DOI: 10.4239/wjd.v7.i17.412 [PubMed: 27660698]

Saha AK, Xu XJ, Lawson E, Deoliveira R, Brandon AE, Kraegen EW, Ruderman NB. Downregulation of AMPK accompanies leucine- and glucose-induced increases in protein synthesis and insulin resistance in rat skeletal muscle. Diabetes. 2010; 59:2426–2434. DOI: 10.2337/db09-1870 [PubMed: 20682696]

Sando KR, Barboza J, Willis C, Taylor J. Recent diabetes issues affecting the primary care clinician. South Med J. 2011; 104:456–461. DOI: 10.1097/SMJ.0b013e318213e92b [PubMed: 21886036]

Sena CM, Pereira AM, Carvalho C, Fernandes R, Seiça RM, Oliveira CR, Moreira PI. Type 2 diabetes aggravates Alzheimer's disease-associated vascular alterations of the aorta in mice. J Alzheimers Dis JAD. 2015; 45:127–138. DOI: 10.3233/JAD-141008 [PubMed: 25471187]

Sheen YJ, Sheu WHH. Association between hypoglycemia and dementia in patients with type 2 diabetes. Diabetes Res Clin Pract. 2016; 116:279–287. DOI: 10.1016/j.diabres.2016.04.004 [PubMed: 27321346]

Steen E, Terry BM, Rivera EJ, Cannon JL, Neely TR, Tavares R, Xu XJ, Wands JR, de la Monte SM. Impaired insulin and insulin-like growth factor expression and signaling mechanisms in Alzheimer's disease--is this type 3 diabetes? J Alzheimers Dis JAD. 2005; 7:63–80. [PubMed: 15750215]

Stoica L, Zhu PJ, Huang W, Zhou H, Kozma SC, Costa-Mattioli M. Selective pharmacogenetic inhibition of mammalian target of Rapamycin complex I (mTORC1) blocks long-term synaptic plasticity and memory storage. Proc Natl Acad Sci U S A. 2011; 108:3791–3796. DOI: 10.1073/pnas.1014715108 [PubMed: 21307309]

Stuart CA, Howell MEA, Cartwright BM, McCurry MP, Lee ML, Ramsey MW, Stone MH. Insulin resistance and muscle insulin receptor substrate-1 serine hyperphosphorylation. Physiol Rep. 2014; :2.doi: 10.14814/phy2.12236

Sun XJ, Liu F. Phosphorylation of IRS proteins Yin-Yang regulation of insulin signaling. Vitam Horm. 2009; 80:351–387. DOI: 10.1016/S0083-6729(08)00613-4 [PubMed: 19251044]

Talbot K, Wang HY, Kazi H, Han LY, Bakshi KP, Stucky A, Fuino RL, Kawaguchi KR, Samoyedny AJ, Wilson RS, Arvanitakis Z, Schneider JA, Wolf BA, Bennett DA, Trojanowski JQ, Arnold SE. Demonstrated brain insulin resistance in Alzheimer's disease patients is associated with IGF-1 resistance, IRS-1 dysregulation, and cognitive decline. J Clin Invest. 2012; 122:1316–1338. DOI: 10.1172/JCI59903 [PubMed: 22476197]

Tanti JF, Jager J. Cellular mechanisms of insulin resistance: role of stress-regulated serine kinases and insulin receptor substrates (IRS) serine phosphorylation. Curr Opin Pharmacol. 2009; 9:753–762. DOI: 10.1016/j.coph.2009.07.004 [PubMed: 19683471]

Thornton C, Bright NJ, Sastre M, Muckett PJ, Carling D. AMP-activated protein kinase (AMPK) is a tau kinase, activated in response to amyloid β-peptide exposure. Biochem J. 2011; 434:503–512. DOI: 10.1042/BJ20101485 [PubMed: 21204788]

Vandal M, White PJ, Chevrier G, Tremblay C, St-Amour I, Planel E, Marette A, Calon F. Age-dependent impairment of glucose tolerance in the 3xTg-AD mouse model of Alzheimer's disease. FASEB J. 2015; 29:4273–4284. DOI: 10.1096/fj.14-268482 [PubMed: 26108977]

Velazquez R, Shaw DM, Caccamo A, Oddo S. Pim1 inhibition as a novel therapeutic strategy for Alzheimer's disease. Mol Neurodegener. 2016; :11.doi: 10.1186/s13024-016-0118-z [PubMed: 26809712]

Vingtdeux V, Davies P, Dickson DW, Marambaud P. AMPK is abnormally activated in tangle- and pre-tangle-bearing neurons in Alzheimer's disease and other tauopathies. Acta Neuropathol (Berl). 2011; 121:337–349. DOI: 10.1007/s00401-010-0759-x [PubMed: 20957377]

Wang C, Liu M, Riojas RA, Xin X, Gao Z, Zeng R, Wu J, Dong LQ, Liu F. Protein kinase C theta (PKCtheta)-dependent phosphorylation of PDK1 at Ser504 and Ser532 contributes to palmitate-induced insulin resistance. J Biol Chem. 2009; 284:2038–2044. DOI: 10.1074/jbc.M806336200 [PubMed: 19047061]

Watson GS, Craft S. Modulation of memory by insulin and glucose: neuropsychological observations in Alzheimer's disease. Eur J Pharmacol. 2004; 490:97–113. DOI: 10.1016/j.ejphar.2004.02.048 [PubMed: 15094077]

Westerman MA, Cooper-Blacketer D, Mariash A, Kotilinek L, Kawarabayashi T, Younkin LH, Carlson GA, Younkin SG, Ashe KH. The relationship between Abeta and memory in the Tg2576 mouse model of Alzheimer's disease. J Neurosci Off J Soc Neurosci. 2002; 22:1858–1867.

White MF. Insulin signaling in health and disease. Science. 2003; 302:1710–1711. DOI: 10.1126/science.1092952 [PubMed: 14657487]

Wiseman FK, Al-Janabi T, Hardy J, Karmiloff-Smith A, Nizetic D, Tybulewicz VLJ, Fisher EMC, Strydom A. A genetic cause of Alzheimer disease: mechanistic insights from Down syndrome. Nat Rev Neurosci. 2015; 16:564–574. DOI: 10.1038/nrn3983 [PubMed: 26243569]

Yarchoan M, Arnold SE. Repurposing diabetes drugs for brain insulin resistance in Alzheimer disease. Diabetes. 2014; 63:2253–2261. DOI: 10.2337/db14-0287 [PubMed: 24931035]

Yarchoan M, Toledo JB, Lee EB, Arvanitakis Z, Kazi H, Han LY, Louneva N, Lee VMY, Kim SF, Trojanowski JQ, Arnold SE. Abnormal serine phosphorylation of insulin receptor substrate 1 is associated with tau pathology in Alzheimer's disease and tauopathies. Acta Neuropathol (Berl). 2014; 128:679–689. DOI: 10.1007/s00401-014-1328-5 [PubMed: 25107476]

Zhang X, Tang S, Zhang Q, Shao W, Han X, Wang Y, Du Y. Endoplasmic reticulum stress mediates JNK-dependent IRS-1 serine phosphorylation and results in Tau hyperphosphorylation in amyloid β oligomer-treated PC12 cells and primary neurons. Gene. 2016; 587:183–193. DOI: 10.1016/j.gene.2016.05.018 [PubMed: 27185631]

Zhang Y, Zhou B, Deng B, Zhang F, Wu J, Wang Y, Le Y, Zhai Q. Amyloid-β induces hepatic insulin resistance in vivo via JAK2. Diabetes. 2013; 62:1159–1166. DOI: 10.2337/db12-0670 [PubMed: 23223021]

Zhang Y, Zhou B, Zhang F, Wu J, Hu Y, Liu Y, Zhai Q. Amyloid-β Induces Hepatic Insulin Resistance by Activating JAK2/STAT3/SOCS-1 Signaling Pathway. Diabetes. 2012; 61:1434–1443. DOI: 10.2337/db11-0499 [PubMed: 22522613]

Zilliox LA, Chadrasekaran K, Kwan JY, Russell JW. Diabetes and Cognitive Impairment. Curr Diab Rep. 2016; 16:87.doi: 10.1007/s11892-016-0775-x [PubMed: 27491830]

Highlights

- Type 2 diabetes is a risk factor for Alzheimer's disease (AD).
- In two mouse models of AD (Tg2576 and 3xTg-AD), we report an age-dependent progression of CNS insulin resistance that precedes peripheral insulin resistance.
- Additionally, we find that brain energy metabolism is differentially altered in both mouse models, with the 3xTg-AD mice showing more extensive changes.
- Collectively, our data suggest that early AD may reflect engagement of different signaling networks that influence CNS metabolism, which in-turn alter peripheral insulin signaling.

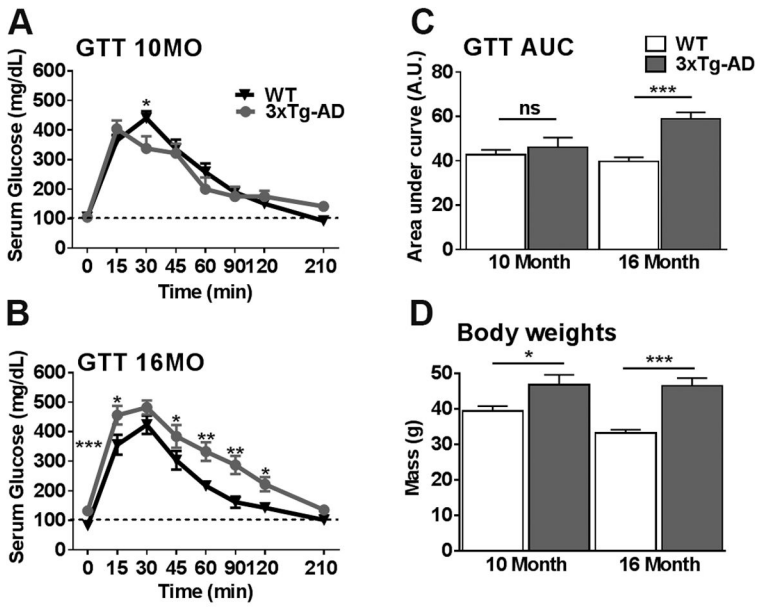

Figure 1. 3xTg-AD mice show an age-dependent onset of peripheral insulin resistance

3xTg-AD and WT mice were given a glucose tolerance test. **(A)** At 10 months of age, a repeated measures ANOVA revealed no significant effect of Genotype ($F_{(1, 28)} = 0.026$, $p > 0.05$), however there was a significant Genotype x Time interaction ($F_{(1, 28)} = 0.0032$, $p < 0.05$). Interestingly the interaction was the result of the WT mice showing a significantly elevated serum glucose mg/DL level compared to 3xTg-AD mice 30 mins after sucrose injection ($p < 0.05$). No other time points were significant. **(B)** At 16 months of age, the repeated measures ANOVA revealed a significant main effect of Genotype ($F_{(1, 28)} = 17.183$, $p < 0.001$) and a significant Genotype x Time interaction ($F_{(1, 28)} = 54.699$, $p < 0.0001$). 3xTg-AD mice showed a significantly elevated serum glucose mg/DL level at fasting (0 mins; $p < 0.0001$) and 15 ($p < 0.05$), 45 ($p < 0.05$), 60 ($p < 0.01$), 90 ($p < 0.01$) and 120 mins ($p < 0.05$) after sucrose injection compared to WT mice. **(C)** Area under the curve (AUC) analysis for glucose revealed no differences at 10 months of age ($t_{(28)} = 0.470$, $p > 0.05$). At 16 months of age, a highly significant student's t-test revealed that 3xTg-AD have a higher glucose AUC compared to WT mice ($t_{(28)} = 27.322$, $p < 0.0001$). **(D)** 3xTg-AD mice weight is significantly higher at 10 ($t_{(28)} = 4.883$, $p < 0.05$) and 16 months of age ($t_{(28)} = 27.634$, $p < 0.0001$) relative to their age-matched WT counterparts. Error bars represent mean ± SEM. *$p < 0.05$, **$p < 0.01$, ***$p < 0.001$. (n = 15/genotype/age).

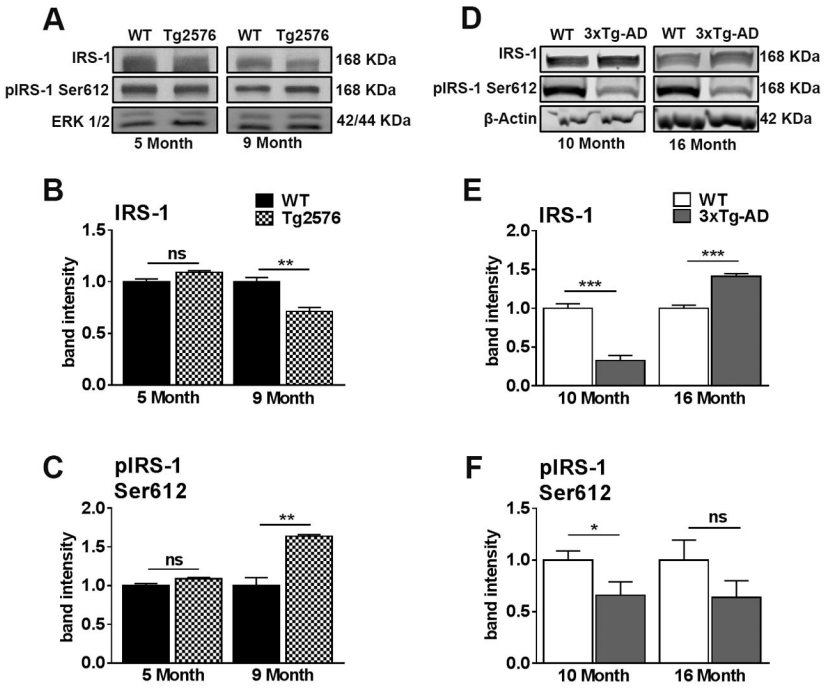

Figure 2. Tg2576 and 3xTg-AD mice show an age-dependent dysregulation of insulin receptor substrate 1 (IRS-1) in the brain

(A) Representative western blots of protein extracted from both 5- and 9-month-old Tg2576 and WT mice. Blots were probed with the indicated antibodies. **(B)** The key mediator of IR activation, IRS-1, is down-regulated in 9-month-old Tg2576 compared to WT mice ($t_{(10)} = 5.245$, $p < 0.01$). **(C)** Inhibitory Ser612 phosphorylation is elevated in 9-month-old Tg2576 mice compared to WT mice ($t_{(10)} = 6.016$, $p < 0.01$). **(D)** Representative western blots of protein extracted from both 10- and 16-month-old 3xTg-AD and age-matched WT mice. **(E)** 10-month-old 3xTg-AD mice show a significant reduction of IRS-1 compared to WT mice ($t_{(10)} = 60.670$, $p < 0.0001$). On the contrary, 16-month-old 3xTg-AD mice show a significant increase in total IRS-1 levels compared to WT mice ($t_{(10)} = 58.765$, $p < 0.0001$). **(F)** 10-month-old 3x-TgAD mice show a significant reduction of pIRS-1 at Ser612 compared to WT mice ($t_{(10)} = 4.772$, $p < 0.05$). Quantitative analyses of the blots obtained by normalizing the quantity of a specific protein with its loading control. Error bars represent mean ± SEM. *$p < 0.05$, **$p < 0.01$, ***$p < 0.001$. (n = 6/genotype/age).

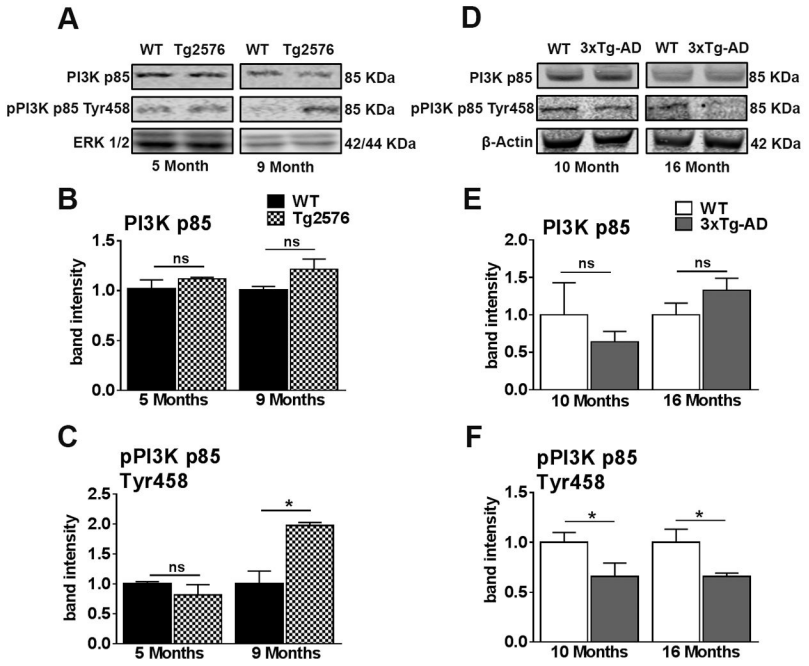

Figure 3. Tg2576 and 3xTg-AD mice show an age-dependent dysregulation of PI3K in the brain

(A) Representative western blots of protein extracted from 5- and 9-month-old Tg2576 and WT mice. Blots were probed with the indicated antibodies. **(B)** PI3K p85, a downstream target of IRS-1, was not significantly different between WT and Tg2576 mice at both ages analyzed. (**C)** The levels of PI3K p85 phosphorylated at Tyr485 were significantly increased in 9-month-old Tg2576 mice compared to WT mice ($t_{(10)} = 4.429$ $p < 0.05$). **(D)** Representative western blots of protein extracted from both 10- and 16-month-old 3xTg-AD and age-matched WT mice. **(E)** PI3K p85 levels were not significantly different between WT and 3xTg-AD mice at both ages analyzed **(F)** 10- and 16-month-old 3xTg-AD mice show a significant reduction in the levels of pPI3K p85 phosphorylated at Tyr485 compared to age-matched WT mice ($t_{(10)} = 6.681$, $p < 0.05$ and $t_{(10)} = 7.997$, $p < 0.05$, respectively). Quantitative analyses of the blots was obtained by normalizing the quantity of a specific protein with its loading control. Error bars represent mean ± SEM. *$p < 0.05$, **$p < 0.01$, ***$p < 0.001$. (n = 6/genotype/age).

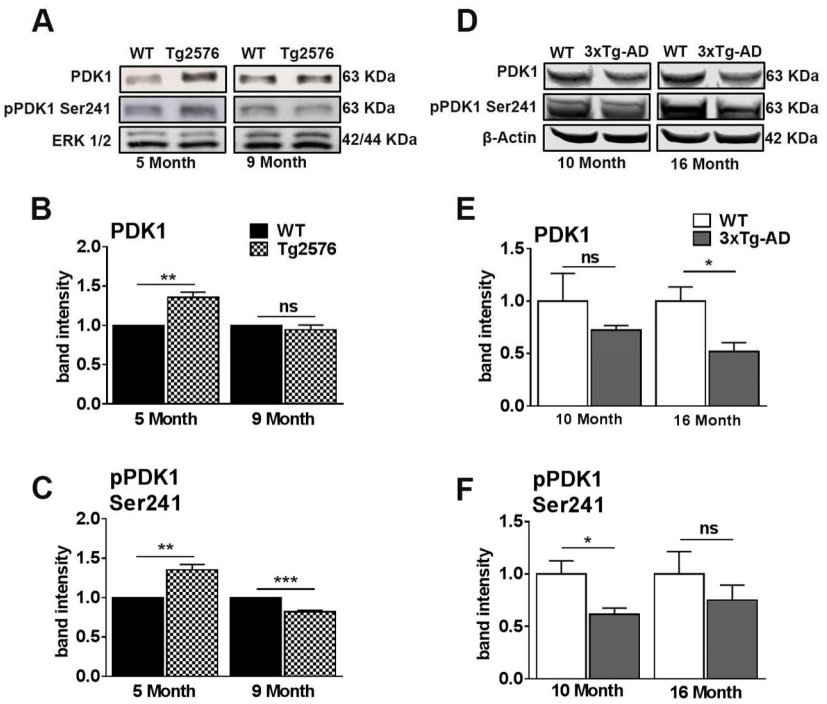

Figure 4. PDK1 activity is dysregulated prior to the onset of peripheral insulin resistance in Tg2576 and 3xTg-AD mice

(A) Representative western blots of protein extracted from both 5- and 9-month-old Tg2576 and WT mice. Blots were probed with the indicated antibodies. **(B)** PDK, a downstream kinase of insulin receptor activation, was up regulated in 5-month-old Tg2576 ($t_{(10)} = 5.13$, $p < 0.01$), but not 9-month-old compared to WT. **(C)** pPDK is up regulated in 5-month-old and downregulated in 9-month-old Tg2576 mice compared to WT mice ($t_{(10)} = 5.13$, $p < 0.01$ and $t_{(10)} = 8.647$, $p < 0.001$ for 5- and 9-month-old, respectively). **(D)** Representative western blots of protein extracted from both 10- and 16-month-old 3xTg-AD and WT mice. **(E)** 10-month-old 3xTg-AD mice show no significant differences in total PDK1 levels compared to age-matched WT mice. At 16 months of age, 3xTg-AD mice show a significant reduction in total PDK levels compared to WT mice ($t_{(10)} = 8.987$, $p < 0.05$). **(F)** 10-month-old 3xTg-AD mice show a significant reduction of pPDK1 at Ser 241 compared to age-matched WT mice ($t_{(10)} = 7.722$, $p < 0.05$). No significant difference for 16-month-old 3xTg-AD mice. Quantitative analyses of the blots obtained by normalizing the quantity of a specific protein with its loading control. Error bars represent mean ± SEM. *$p < 0.05$, **$p < 0.01$, ***$p < 0.001$. n = 6/genotype/age.

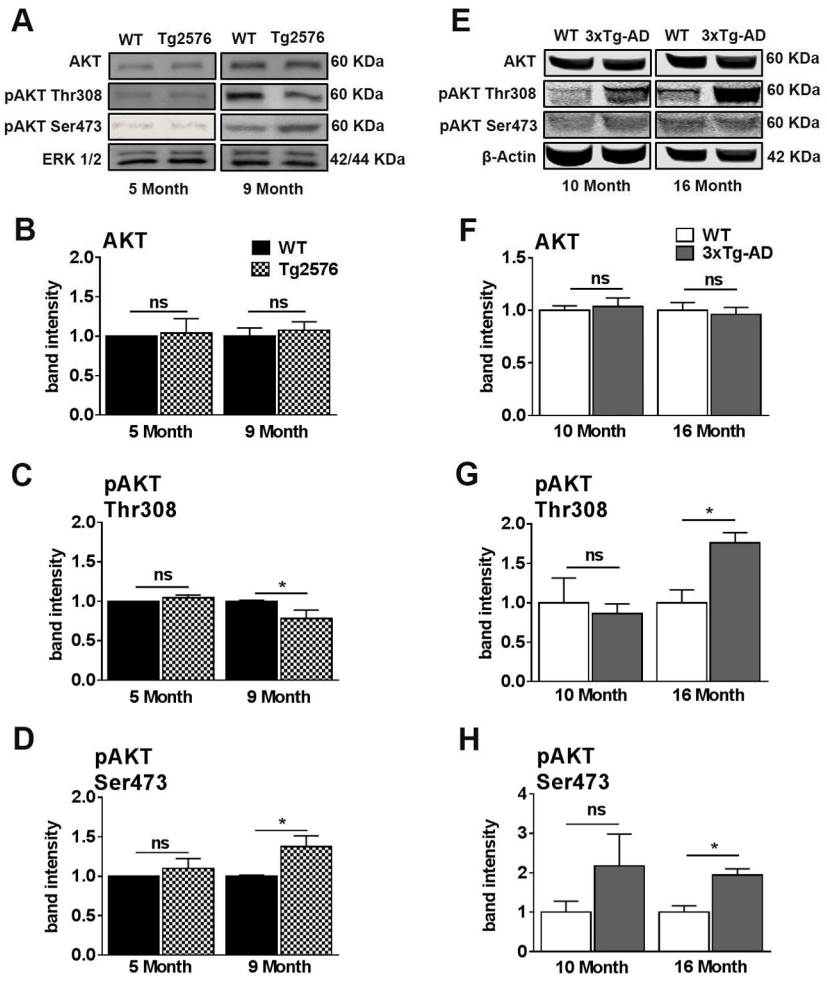

Figure 5. AKT activity is dysregulated concomitantly with peripheral insulin resistance in Tg2576 and 3xTg-AD mice

(A) Representative western blots of protein extracted from both 5- and 9-month-old Tg2576 and WT mice. Blots were probed with the indicated antibodies. **(B)** AKT levels were not significant difference between 5- and 9-month-old WT and Tg2576 mice. **(C)** Phosphorylation of AKT at Thr308 was significantly downregulated in 9-month-old Tg2576 compared to WT mice ($t_{(10)} = 2.661$, $p < 0.05$). **(D)** AKT was hyper-phosphorylated at Ser473 in 9-month-old Tg2576 compared to WT mice ($t_{(10)} = 2.710$, $p < 0.05$). **(E)** Representative western blots of protein extracted from both 10- and 16-month-old 3xTg-AD and WT mice. **(F)** No significant differences were found between 10-month-old WT and 3xTg-AD mice and between 16-month-old WT and 3xTg-AD mice for AKT. **(G)** No significant differences were found between 10-month-old WT and 3xTg-AD mice for pAKT at Thr308. At 16 months of age, 3xTg-AD mice show a significant elevation in pAKT at Thr308 compared to WT mice ($t_{(10)} = 8.441$, $p < 0.05$). **(H)** No significant differences for pAKT at Ser473 between 10-month-old WT and 3xTg-AD mice. At 16 months of age, 3xTg-AD mice show a significantly elevated level of pAKT at Ser473 compared to WT mice ($t_{(10)} = 7.989$, $p < 0.05$). Quantitative analyses of the blots obtained by normalizing the

quantity of a specific protein with its loading control. Error bars represent mean ± SEM. *p < 0.05, **p < 0.01, ***p < 0.001. n = 6/genotype/age.

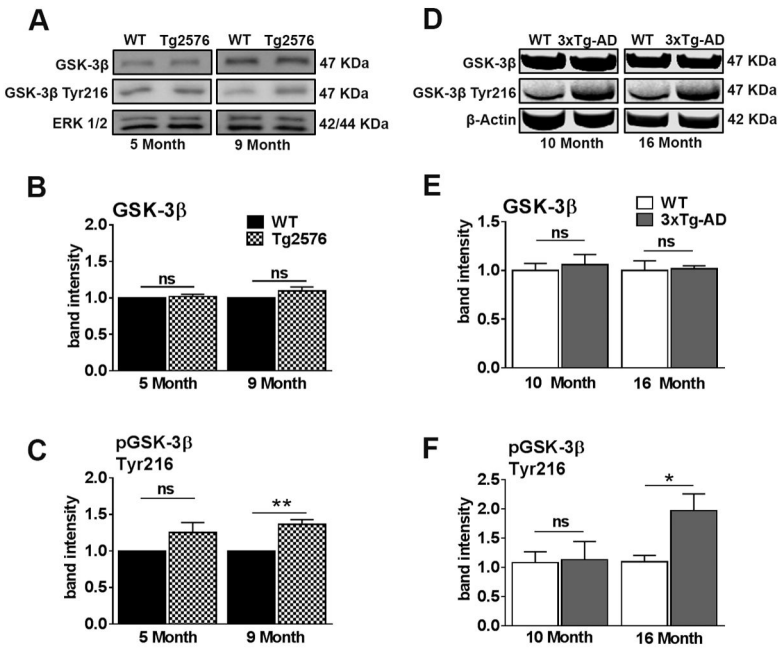

Figure 6. GSK-3β activity is dysregulated concomitantly with peripheral insulin resistance in Tg2576 and 3xTg-AD mice

(A) Representative western blots of protein extracted from both 5- and 9-month-old Tg2576 and WT mice. Blots were probed with the indicated antibodies. **(B)** GSK-3β levels were unaltered at 5-month-old and 9-month-old in Tg2576 mice compared to WT mice. **(C)** The excitatory phosphorylation site of GSK-3β at Tyr216 was enhanced in 9-month-old Tg2576 mice compared to WT mice ($t_{(10)} = 5.390$, $p < 0.01$). **(D)** Representative western blots of protein extracted from both 10- and 16-month-old 3xTg-AD and WT mice. **(E)** No significant differences between 10-month-old WT and 3xTg-AD mice and between 16-month-old WT and 3xTg-AD mice for GSK-3β. **(F)** No significant differences for pGSK-3β at Tyr216 were detected between 10-month-old WT and 3xTg-AD mice. 16-month-old 3xTg-AD mice show significantly elevated levels of pGSK-3β at Tyr216 compared to WT mice ($t_{(10)} = 5.125$, $p < 0.05$). Quantitative analyses of the blots obtained by normalizing the quantity of a specific protein with its loading control. Error bars represent mean ± SEM. *p<0.05, **p<0.01, ***p<0.001. n = 6/genotype/age.

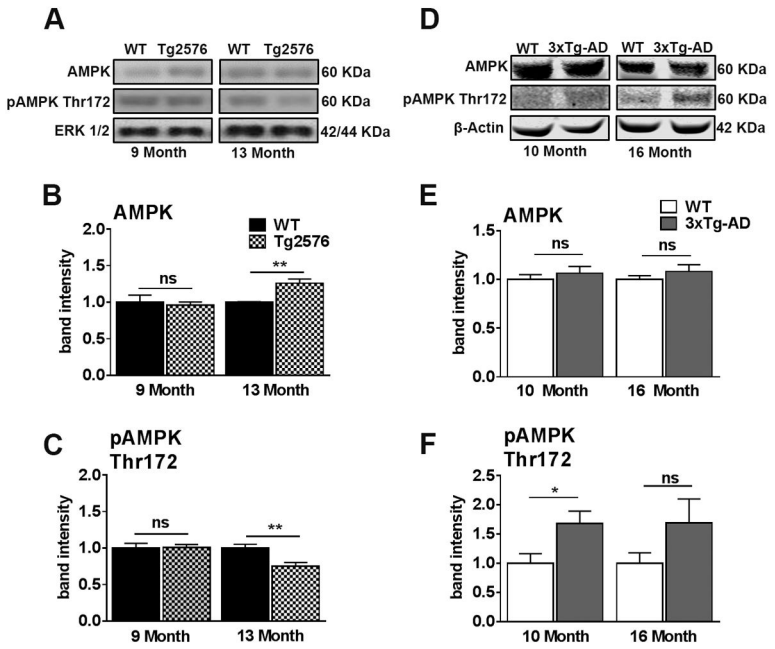

Figure 7. AMPK is dysregulated in 13-month-old Tg2576 and 10-month-old 3xTg-AD mice

(A) Representative western blots of protein extracted from both 9- and 13-month-old Tg2576 and WT mice. Blots were probed with the indicated antibodies. **(B)** Total AMPK is up regulated in 13-month-old, but not 9-month-old Tg2576 mice ($t_{(10)} = 4.654$, $p < 0.001$). **(C)** Phosphorylation activation of AMPK is decreased in 13-month-old, but not 9-month-old Tg2576 mice ($t_{(10)} = 3.410$, $p < 0.01$). **(D)** Representative western blots of protein extracted from both 10- and 16-month-old 3xTg-AD and WT mice. **(E)** No significant differences in AMPK between 10-month-old WT and 3xTg-AD mice and between 16-month-old WT and 3xTg-AD mice. **(F)** pAMPK at Thr172 was significantly elevated in 3xTg-AD mice compared to WT mice at 10 months of age ($t_{(10)} = 6.425$, $p < 0.05$). No significant differences for pAMPK at Thr172 between16-month-old WT and 3xTg-AD mice. Quantitative analyses of the blots obtained by normalizing the quantity of a specific protein with its loading control. Error bars represent mean ± SEM. *$p < 0.05$, **$p < 0.01$, ***$p < 0.001$. (n = 6/genotype/age).

Neurobiol Aging. Author manuscript; available in PMC 2018 October 01.

Table 1

Peripheral insulin resistance in 9-month-old Tg2576 and 16-month-old 3xTg-AD mice compared to age matched WT mice.

Glucose Tolerance Test								
Tg2576 vs. WT (Rodriguez-Rivera et al., 2011)								
Age	**Fasting**	**15min**	**30min**	**45min**	**60min**	**90min**	**120min**	**210min**
5 Months	ns	ns	ns	ns	ns	ns	ns	ns
9 Months	ns	↑, **	↑, ***	↑, **	↑, **	↑, *	ns	ns
3xTg-AD vs. WT (Fig. 1)								
Age	Fasting	15min	30min	45min	60min	90min	120min	210min
10 Months	ns	ns	↓, *	ns	ns	ns	ns	ns
16 Months	↑, ***	↑, *	ns	↑, *	↑, **	↑, **	↑, *	ns

Arrows indicate a significant increase (↑) or decrease (↓) in glucose level over age-matched WT.

Abbreviations: ns = non-significant, GTT = Glucose tolerance test.

* $p < 0.05$,

** $p < 0.01$,

*** $p < 0.001$.